JACS
JOURNAL OF THE AMERICAN CHEMICAL SOCIETY
Communication
pubs.acs.org/JACS

Multivariable Modular Design of Pore Space Partition

Xiang Zhao,[†] Xianhui Bu,*[,‡] Edward T. Nguyen,[‡] Quan-Guo Zhai,[†] Chengyu Mao,[†] and Pingyun Feng*[,†]

[†]Department of Chemistry, University of California, Riverside, California 92521, United States

[‡]Department of Chemistry and Biochemistry, California State University Long Beach, 1250 Bellflower Boulevard, Long Beach, California 90840, United States

Supporting Information

ABSTRACT: Pore space partition, especially the one using C_3-symmetric 2,4,6-tri(4-pyridyl)-1,3,5-triazine as pore-partition agent in MIL-88 type (the **acs** net), has been shown to dramatically enhance CO_2 uptake to near-record values. The continued advance in property engineering via pore space partition would depend on intelligent design of both framework components and pore-partition agent. Here, we report a new advance in the design of pore-partition agent by demonstrating a symmetry-guided pathway to develop a large variety of di- and trinuclear 1,2,4-triazolate-based clusters for use as pore-partition agent. The use of metal−organic clusters (instead of organic ligands) as pore-partition agent gives rise to many new pore-partitioned materials with huge compositional variety. The full assembly involves the simultaneous formation of two separate coordination architectures (i.e., the 3-D **acs** framework and 0-D triazolate clusters) and the eventual welding between the **acs** framework and triazolate clusters. The wide range of new compositions and structures provides a high degree of tunability in gas sorption properties.

The synthesis of new crystalline porous materials is a cornerstone for advanced applications.[1−12] Recently we reported a pore-space-partition strategy involving the insertion of C_3-symmetric 2,4,6-tri(4-pyridyl)-1,3,5-triazine (**tpt**) ligand into MIL-88-type structures (the **acs** net) to generate a new framework type, denoted **pacs** (*partitioned* **acs**) (Figure 1a).[13,14] The key to achieve **pacs** structures is the use of a pore-partition agent whose symmetry (C_3-symmetric) and size match well with the parent framework. We further found that the symmetry matching is a more important design parameter than the size matching because the softness of MIL-88 type structures relaxes the size-matching requirement between its channel size and the size of pore-partition agent.

Compared to previously reported pore-partitioned examples,[10] our ligand-insertion method on the **acs** platform introduces modularity because individual control over parent framework and pore-partition agent can be achieved. Such modularity leads to a **pacs**-based platform whose multiple modules can be separately replaced or tuned to generate practically numerous distinct new MOFs under the same building regime. In this work, we demonstrate the power of this platform by revealing new members of the **pacs** family prepared through synthesis routes that are distinctly different from that used for making members of **tpt-pacs**.

The synthesis of **tpt-pacs** relies on metal-free organic ligands as pore-partition agent. While organic ligands can be diverse, even more diversity can be achieved by combining organic and inorganic units. Here, we report a symmetry-guided cooperative coordination strategy to develop new **pacs** members using a variety of in situ formed, C_3-symmetric, di- or trinuclear 1,2,4-triazolate clusters as pore-partition agent. Compared to **tpt-pacs**, this new strategy has the following features introduced by pore-partition agent: (i) it uses much cheaper and readily available azolate ligands that are more diverse than tpt-type ligands, (ii) it introduces two extra types of metal clusters (i.e., di- and trinuclear triazolate clusters) that permits greater property engineering (including catalytic or magnetic), and (iii) it introduces a novel method of controlling the type, location, and orientation of open metal sites through pore-partition agent (i.e., triazolate clusters) as compared to those located on the primary framework.

While our new design concept is simple and modular, the actual synthesis entails a complex multicomponent system. The full assembly involves simultaneous formation of two separate coordination architectures (i.e., the 3-D **acs** type metal−organic framework and 0-D di- or trinuclear metal−organic clusters) in a dual-metal and dual-ligand mixture and the eventual welding between them. To achieve the desired goal, all the components have to work cooperatively. In this work, we have explored a large variety of chemical combinations, leading to a new generation of **pacs** family of materials with highly tunable properties.

Specifically, we demonstrate the use of various 1,2,4-triazolate (**trz**) clusters as pore-partition agent. There are two known types of triazolate clusters with C_3 symmetry, a paddlewheel dimer and a planar trimer.[15] As shown here for the first time, both clusters can be used for pore-partition agent, leading to two families of materials denoted as **trz-pacs-D** (Figure 1c, D = dimer) and **trz-pacs-T** (Figure 1d, T = trimer). In addition, a new type of **pacs** materials prepared by a new mechanism (through bonding between pyridyl sites on the **acs** framework and metal ions at the channel centers, Figure 1b,e) are also presented here. All structures were determined by single-crystal X-ray diffraction.

The **trz-pacs-D** family has a general formula of $[(\mathbf{M1})_3\mathrm{O}(\mathbf{L1})_3][(\mathbf{M2})_2(\mathbf{L2})_3\mathrm{X}_6]$ (X = H_2O or Cl^-), where $[(\mathbf{M1})_3\mathrm{O}(\mathbf{L1})_3]$ represents the formula of the **acs** net and $[(\mathbf{M2})_2(\mathbf{L2})_3\mathrm{X}_6]$ is the formula of triazolate dimer (Figure 1c). In the **acs** framework, **M1** is a metal or a combination of different metal ions capable of forming trimers (in this work, only Fe, In,

Received: July 30, 2016
Published: November 14, 2016

DOI: 10.1021/jacs.6b07901
J. Am. Chem. Soc. 2016, 138, 15102−15105

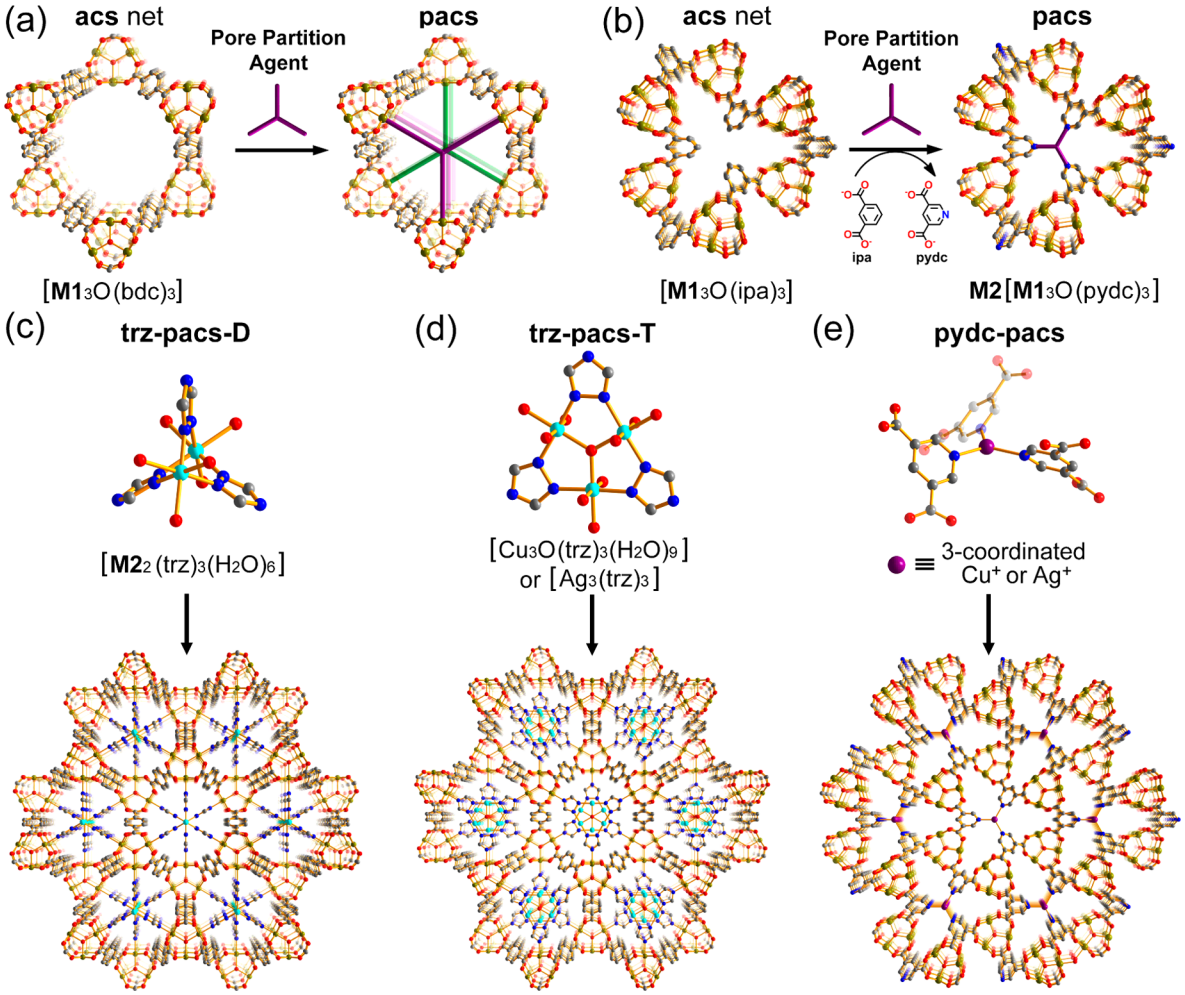

Figure 1. (Top) Two schemes to create **pacs** structures: (a) through framework open metal sites and (b) through framework open pyridyl site on 3,5-dicarboxylpyridine. Structures of pore-partition agents (middle) and 3-D partitioned frameworks (bottom) of (c) **trz-pacs-D**, (d) **trz-pacs-T** and (e) **pydc-pacs**. Color code: gold, **M1** from **acs** net; cyan, **M2** from pore-partition agent; red, O; blue, N; gray, C. ipa = isophthalate.

and In/Co are selected to make the scope manageable) and **L1** is a dicarboxylate such as terephthalate (bdc) or its derivatives. In the triazolate dimer, **M2** is a metal or metal combinations that can form triazolate dimers (here, In, Zn, Ni, Co, Fe, Mn, Mg, and In/Co are chosen) and **L2** refers to 1,2,4-triazolate (trz) or its derivatives. Some **M2**/**L2** combinations (e.g., indium triazolate dimer) achieved here were not known in the literature, suggesting that the co-assembly between the **acs** net and pore-partition agent has synergistic effects and can stabilize clusters previously not known to exist.

Unlike **tpt-pacs** with planar and stretched organic pore-partition agent, dinuclear triazolate clusters in **trz-pacs-D** are nonplanar and quite compact in size because two metal ions are aligned along the channel direction. The overall size of the dimer, as projected onto *ab* plane is smaller than tpt, leading to a smaller *a* axis (∼14.0 Å in **trz-pacs-D** vs ∼16.7 Å in **tpt-pacs**).

The **trz-pacs-T** family is made from planar trinuclear triazolate clusters (Figure 1d). Its *a* axis (∼15.8 Å) is larger than that in **trz-pacs-D**, but smaller than that in **tpt-pacs**. So far, two new structures have been made with Ag and Cu in planar trimers. One is heterometallic In/Ag structure with the formula $[In_3O(bdc)_3]$-$[Ag_3(trz)_3](NO_3)$. Another is the heterometallic Fe/Cu structure with the formula $[Fe_3O(dhbdc)_3][Cu_3O$-$(trz)_3(OH)_2(H_2O)_7]$. While copper triazolate cluster has a μ_3-O core, silver trimer has an empty core.

In the three **pacs** families (**tpt-pacs**, **trz-pacs-D**, and **trz-pacs-T**), three pyridyl groups used for pore space partition are located on pore-partition agent inside the channel. Herein we show a new mechanism for pore space partition (Figure 1b). With this new mechanism, the pyridyl functionality is located on the **acs** framework made from 3,5-dicarboxylpyridine (pydc), and metal ions (i.e., Cu^+ or Ag^+) capable of adopting C_3-symmetric coordination geometry (Figure 1e) are used as pore-partition agent. Two new structures in heterometallic In/Ag and Mg/Cu compositions were synthesized with the formula of $Ag[In_3O$-$(pydc)_3](NO_3)_2$ and $Cu[Mg_3(OH)(pydc)_3]$, respectively.

It is interesting to compare the four **pacs** families. While **pydc-pacs** adopts a three-nodal 3,3,6-connected net, **tpt-pacs**, **trz-pacs-D**, and **trz-pacs-T** share the same two-nodal 3,9-connected net (Figure S11). Importantly, there is a systematic trend in the number of metal ions needed for pore-partition agent. While **tpt-pacs** requires no metal ions for pore-partition agent, **pydc-pacs**, **trz-pacs-D**, and **trz-pacs-T** require one, two, and three metals, respectively.

The impact of our different pore space partition methods on open metal sites (**OMS**) is dramatic because both location, orientation, and density of OMS are affected. In addition, greater hydrothermal stability can be achieved by shifting open-metal sites from the framework metal sites to the triazolate cluster at the channel center (Figure S24). In **tpt-pacs**, all open metal sites

DOI: 10.1021/jacs.6b07901
J. Am. Chem. Soc. 2016, 138, 15102−15105

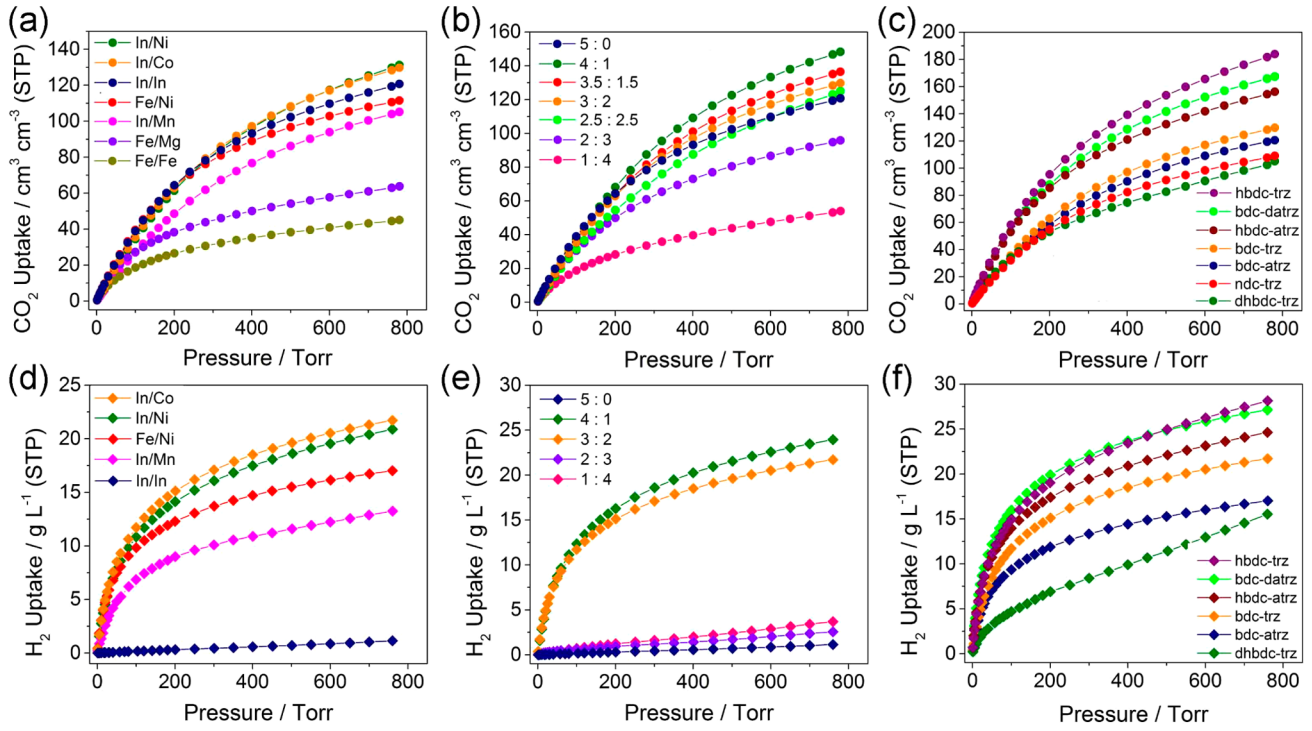

Figure 2. Gas sorption studies on **trz-pacs-D** structure platform. (a–c) Volumetric CO_2 uptake measured at 273 K. (d–f) Volumetric H_2 uptake measured at 77 K, for **trz-pacs-D** compounds with three different sets of composition control, which are $[\mathbf{M1}_3O(bdc)_3][\mathbf{M2}_2(trz)_3X_6]$ in different **M1**/**M2** combinations (except for Fe/Fe, Fe/Mg, Fe/Ni samples, in which hbdc was used instead of bdc), $[M_3O(bdc)_3][M_2(trz)_3X_6]$ (**M** = In, Co, or In/Co mixture) in different In/Co ratios, and $[In_3O(\mathbf{L1})_3][Co_2(\mathbf{L2})_3X_6]$ in different **L1**/**L2** ligand combinations, respectively (X = H_2O, Cl^-, or their combinations).

on the **acs** framework are occupied by pore-partition agent, which is also the case for **trz-pacs-D** and **trz-pacs-T** platforms. However, the design method for **trz-pacs** platforms compensates such loss with OMS on pore-partition agent. As a result, **trz-pacs-D** (with bdc ligand) has a maximum of 12 OMS per unit cell (or ~3.9 OMS/nm^3), and **trz-pacs-T** (also with bdc ligand) has a maximum of 18 OMS per unit cell and the OMS density can reach as high as ~5.0 OMS/nm^3. For **pydc-pacs**, the value is ~2.5 OMS/nm^3. In comparison, the OMS density in MOF-74 and HKUST-1 is ~4.5 OMS/nm^3 and 2.6 OMS/nm^3, respectively. Finally, the Platon calculation shows ~49.2% of the free pore volume in **trz-pacs-T** (without coordinated solvent) and ~42.7% in **trz-pacs-D**, in comparison with ~47.5% in **tpt-pacs** (based on the same bdc ligand). For all members of the **pacs** platform, the free pore volume can have a large range due to the tunability in **L1** and **L2** ligands.

A prominent feature of the **pacs** platform is huge compositional tunability offered by their modular building schemes. Both **trz-pacs-D** and **trz-pacs-T** are tunable in all their components, **M1**, **M2**, **L1**, and **L2** (Table S1), which is made easy and practical because all these components are in common chemical forms (simple dicarboxylate and triazolate, trigonal prismatic trimers and paddlewheel dimers). The diversity of metal species in **trz-pacs** can not only be achieved in trigonal prismatic clusters in **acs** net but also in triazolate clusters. Using **trz-pacs-D** as an example, in this study, we have obtained this type (with a general formula as $[(\mathbf{M1})_3O(bdc)_3][(\mathbf{M2})_2(trz)_3X_6]$, X = H_2O or Cl^-) in eight different **M1**/**M2** combinations (In/Zn, In/Mn, In/Co, In/Ni, In/In, Fe/Mg, Fe/Ni Fe/Fe, hbdc was used in Fe-containing compounds) (Table S2 and Figure S18). Considering the solvent on **M2** is potentially removable, the abundant choice of **M2** makes **trz-pacs-D** an ideal platform to probe how gas sorption properties can be tuned by metal types. Finally, the various combinations between dimers and trimers could produce an enormous variety of heterometallic inorganic compositions on the same platform.

For certain **M1**/**M2** combinations in **trz-pacs-D**, the **M1**/**M2** ratio can be tuned, leading to alloy-like phenomenon on this platform (Table S3). Interestingly, some metal ions (such as In, Ni, Co, Fe, Mn) can form both trigonal prism trimers on the **acs** framework and triazolate dimers on the pore-partition agent. Thus, it is possible to systematically change the ratio between two metals. Here, In/Co was used to demonstrate such tunability. By controlling the In/Co molar ratio in the starting synthesis mixtures (5:0, 4:1. 3.5:1.5, 3:2, 2.5:2.5, 2:3, 1:4), seven compounds were obtained. The energy-dispersive X-ray spectroscopy (EDS) study shows that the In/Co ratio in the crystalline product matches well with the initial ratio in the synthesis (Figure S17).

Another advantage of the **pacs** platform is that both dicarboxylate and triazolate ligands are simple, inexpensive, and modular, which allows easy replacement by their derivatives with different substituents. Meanwhile, **L1** and **L2** ligands play very different structural roles. Thus, **trz-pacs** provides an excellent platform to study the effect of functional groups on gas sorption properties. In this work, we obtained seven different **L1**/**L2** combinations in **trz-pacs-D** (bdc/trz, bdc/atrz, bdc/datrz, hbdc/trz, hbdc/atrz, dhbdc/trz, ndc/trz) at the fixed In:Co ratio of 3:2 (Table S4).

The **trz-pacs-D** family was chosen as the platform for gas sorption studies. Gas sorption properties are studied on samples with different combinations **M1**/**M2** or **L1**/**L2**, as well as on samples with variable **M1**/**M2** ratios. First, CO_2 and H_2 sorption was performed with seven compounds containing different **M1**/

DOI: 10.1021/jacs.6b07901
J. Am. Chem. Soc. 2016, 138, 15102–15105

M2 combinations and two unsubstituted **L1**/**L2** ligands (bdc and trz). Since all these compounds have similar unit cell parameters, it is appropriate to use volumetric uptake capacity for comparison. At 1 atm and 273 K, the CO_2 uptake can be tuned from 44.5 cm^3/cm^3 to 129.7 cm^3/cm^3 in the increasing order of Fe/Fe, Fe/Mg, In/Mn, Fe/Ni, In/In, In/Co, and In/Ni (Figure 2a). The Q_{st} obtained from CO_2 sorption isotherms at 273 and 298 K shows a higher value than Q_{st} in **tpt-pacs** structures (~22 kJ/mol). The Q_{st} at zero loading ranges from 25 to 29 kJ/mol (Figure S23a). These Q_{st} values remain stable with increasing loading. Similarly, H_2 sorption at 77 K also shows a great tunability by varying **M1**/**M2** combination (Figure 2d).

In addition to different **M1**/**M2** combinations, gas sorption performance can be tuned by varying the **M1**/**M2** ratio as shown by **trz-pacs-D** with different In/Co ratios and two unsubstituted **L1**/**L2** ligands (bdc and trz). CO_2 uptake at 1 atm and 273 K increases dramatically with increasing In/Co ratio (from 53.2 cm^3/cm^3 for In/Co ratio at 1:4 to 146.7 cm^3/cm^3 for In/Co ratio of 4:1) (Figure 2b). However, for the all-indium compound (indium in both trimer and dimer), the CO_2 uptake capacity decreases again, compared to the sample with the 4:1 In/Co ratio. Interestingly, the Q_{st} has an opposite trend. The one with the highest sorption capacity (In/Co = 4/1) has the lowest Q_{st} (~24.3 kJ/mol). With decreasing In/Co ratio, the Q_{st} increases slightly to ~32.0 kJ/mol for 1:4 sample. On the other hand, the Q_{st} for all-indium sample falls to ~28.8 kJ/mol (Figure S23b). The effect of the In/Co ratio is even more pronounced on H_2 sorption. While samples with the In/Co 3:2 and 4:1 ratios show a relatively high uptake capacity (21.7 g/L and 24.0 g/L), samples with other three ratios show significantly lower capacity (<~4.0 g/L) (Figure 2e).

Gas sorption properties can also be tuned by **L1**/**L2** combinations. With two $-NH_2$ groups on trz (i.e., **L1**/**L2** = bdc/datrz), the CO_2 sorption at 1 atm and 273 K is increased by 29% from 128.3 cm^3/cm^3 (for bdc/trz) to 165.8 cm^3/cm^3 (for bdc/datrz). Similarly, with one −OH group on bdc (i.e., **L1**/**L2** = hbdc/trz), the value increased 42% to 181.7 cm^3/cm^3 (Figure 2c). Also observed is the enhanced Q_{st} during the entire gas loading process, indicating steadily stronger interaction between the framework and CO_2 when $-NH_2$ and −OH groups are present (Figure S23c). Similar tuning is observed for H_2 sorption (Figure 2f).

In summary, we have introduced new pore space partition strategies, leading to three novel **pacs** series, namely **trz-pacs-D**, **trz-pacs-T**, and **pydc-pacs**. They distinguish themselves from earlier **tpt-pacs** by much richer heterometallic compositions, as well as incorporation of high density of open metal sites. They also demonstrate a modular design principle which will help advance the **pacs** family and pore space partition methods in general. Furthermore, we show **trz-pacs** as a versatile platform capable of encompassing practically numerous chemically distinct materials with tunable properties. We have demonstrated how gas sorption properties can be tuned by multivariable control over their compositions. Such wide range of compositional tunability would allow the modulation of not only gas sorption properties but also many other properties such as catalysis, separation, or magnetic properties, nearly all of which remain to be explored.

■ ASSOCIATED CONTENT

Supporting Information

The Supporting Information is available free of charge on the ACS Publications website at DOI: 10.1021/jacs.6b07901.

Experimental details, Tables S1−S17, and Figures S1−S25 (PDF)

X-ray crystallographic data (CIF)

■ AUTHOR INFORMATION

Corresponding Authors

*xianhui.bu@csulb.edu

*pingyun.feng@ucr.edu

Notes

The authors declare no competing financial interest.

■ ACKNOWLEDGMENTS

The research is supported by the U.S. Department of Energy, Office of Basic Energy Sciences, Division of Materials Sciences and Engineering under Award No. DE-SC0010596 (P.F.).

■ REFERENCES

(1) (a) Furukawa, H.; Cordova, K. E.; O'Keeffe, M.; Yaghi, O. M. *Science* **2013**, *341*, 1230444. (b) Nugent, P.; Belmabkhout, Y.; Burd, S. D.; Cairns, A. J.; Luebke, R.; Forrest, K.; Pham, T.; Ma, S.; Space, B.; Wojtas, L.; Eddaoudi, M.; Zaworotko, M. J. *Nature* **2013**, *495*, 80.

(2) Horcajada, P.; Gref, R.; Baati, T.; Allan, P. K.; Maurin, G.; Couvreur, P.; Férey, G.; Morris, R. E.; Serre, C. *Chem. Rev.* **2012**, *112*, 1232.

(3) Wang, H.; Li, B.; Wu, H.; Hu, T.; Yao, Z.; Zhou, W.; Chen, B. *J. Am. Chem. Soc.* **2015**, *137*, 9963.

(4) Li, B. Y.; Zhang, Z. J.; Li, Y.; Yao, K. X.; Zhu, Y. H.; Deng, Z. Y.; Yang, F.; Zhou, X. J.; Li, G. H.; Wu, H. H.; Nijem, N.; Chabal, Y. J.; Shi, Z.; Feng, S. H.; Li, J. *Angew. Chem., Int. Ed.* **2012**, *51*, 1412.

(5) Hu, T.; Wang, H.; Li, B.; Krishna, R.; Wu, H.; Zhou, W.; Zhao, Y.; Han, Y.; Wang, X.; Zhu, W.; Yao, Z.; Xiang, S.; Chen, B. *Nat. Commun.* **2015**, *6*, 7328.

(6) Sava Gallis, D. F.; Parkes, M. V.; Greathouse, J. A.; Zhang, X. Y.; Nenoff, T. M. *Chem. Mater.* **2015**, *27*, 2018.

(7) Zhang, H.-X.; Liu, M.; Wen, T.; Zhang, J. *Coord. Chem. Rev.* **2016**, *307*, 255.

(8) Fei, H.; Cohen, S. M. *J. Am. Chem. Soc.* **2015**, *137*, 2191.

(9) (a) Deng, H.; Doonan, C. J.; Furukawa, H.; Ferreira, R. B.; Towne, J.; Knobler, C. B.; Wang, B.; Yaghi, O. M. *Science* **2010**, *327*, 846. (b) Wang, L. J.; Deng, H.; Furukawa, H.; Gándara, F.; Cordova, K. E.; Peri, D.; Yaghi, O. M. *Inorg. Chem.* **2014**, *53*, 5881. (c) Zhai, Q.-G.; Bu, X.; Mao, C.; Zhao, X.; Feng, P. *J. Am. Chem. Soc.* **2016**, *138*, 2524. (d) Li, J.-R.; Yu, J.; Lu, W.; Sun, L.-B.; Sculley, J.; Balbuena, P. B.; Zhou, H.-C. *Nat. Commun.* **2013**, *4*, 1538. (e) Wang, B.; Lv, X.-L.; Feng, D.; Xie, L.-H.; Zhang, J.; Li, M.; Xie, Y.; Li, J.-R.; Zhou, H.-C. *J. Am. Chem. Soc.* **2016**, *138*, 6204.

(10) (a) Zheng, S.-T.; Bu, J. T.; Li, Y.; Wu, T.; Zuo, F.; Feng, P.; Bu, X. *J. Am. Chem. Soc.* **2010**, *132*, 17062. (b) Bu, F.; Lin, Q.; Zhai, Q.; Wang, L.; Wu, T.; Zheng, S.; Bu, X.; Feng, P. *Angew. Chem., Int. Ed.* **2012**, *51*, 8538.

(11) (a) Cohen, S. M. *Chem. Rev.* **2012**, *112*, 970. (b) Deria, P.; Mondloch, J. E.; Karagiaridi, O.; Bury, W.; Hupp, J. T.; Farha, O. K. *Chem. Soc. Rev.* **2014**, *43*, 5896. (c) Brozek, C. K.; Dincă, M. *J. Am. Chem. Soc.* **2013**, *135*, 12886.

(12) Zhang, J.; Bu, J.; Chen, S.; Wu, T.; Zheng, S.; Chen, Y.; Nieto, R.; Feng, P.; Bu, X. *Angew. Chem., Int. Ed.* **2010**, *49*, 8876.

(13) (a) Zhao, X.; Bu, X.; Zhai, Q.; Tran, H.; Feng, P. *J. Am. Chem. Soc.* **2015**, *137*, 1396. (b) Zhai, Q.-G.; Bu, X.; Mao, C.; Zhao, X.; Daemon, L. L.; Cheng, Y.; Ramirez-Cuesta, A.; Feng, P. *Nat. Commun.* **2016**, *7*, 13645.

(14) (a) Serre, C.; Millange, F.; Surble, S.; Férey, G. *Angew. Chem., Int. Ed.* **2004**, *43*, 6286. (b) Sudik, A. C.; Côté, A. P.; Yaghi, O. M. *Inorg. Chem.* **2005**, *44*, 2998.

(15) (a) Zhai, Q.-G.; Wu, X.-Y.; Chen, S.-M.; Zhao, Z.-G.; Lu, C.-Z. *Inorg. Chem.* **2007**, *46*, 5046. (b) Zhai, Q.-G.; Lu, C.-Z.; Chen, S.-M.; Xu, X.-J.; Yang, W.-B. *Cryst. Growth Des.* **2006**, *6*, 1393.